JOURNAL OF GUIDANCE, CONTROL, AND DYNAMICS
Vol. 20, No. 4, July–August 1997

Frequency-Domain Optimal Estimator for Wing Rock Models

Szu-Ying Tan*
Aeronautical Research Laboratory, Taichung 40722, Taiwan, Republic of China
and
C. Edward Lan†
University of Kansas, Lawrence, Kansas 66045

An estimation algorithm to identify the nonlinear aerodynamic model in wing rock from the free-to-roll test data is developed. This algorithm is based on an optimal estimation theory with a continuous cost function to minimize the difference between estimates and data. The optimality equations are reformulated in the frequency domain through Beecham–Titchener's averaging technique. The resulting equations are then solved by finite difference. A wing rock model of an 80-deg delta wing is used to verify the method. The method is then applied to a fuselage–vertical tail configuration in a free-to-roll test. The computed response based on the estimated aerodynamic model shows a fair agreement with measured data. Applications of this estimated aerodynamic model in control and aircraft design are discussed. In particular, the necessary additional damping for the suppression of limit-cycle oscillations can be computed. It is shown that unlike an 80-deg delta wing, roll angle feedback to increase the system stiffness can also suppress the body rock of a fuselage–vertical tail configuration.

Nomenclature

A, a = amplitude function
C_1, C_2 = coefficients assumed in Eq. (1) to help numerical convergence
D_i = coefficients of the estimated model equation
d_{11} = $-\mu^2 + \omega^2 + C_1 - C_2\mu$
d_{12} = $2\mu\omega + C_2\omega$
d_{21} = $-2\mu\omega - C_2\omega$
d_{22} = $-\mu^2 + \omega^2 + C_1 - C_2\mu$
F, f = forcing function
G = implicit function
H = Hamiltonian
h_1 = $2\mu\omega - C_2\omega$
h_2 = $-\mu^2 + \omega^2 + C_1 + C_2\mu$
J = cost function
q = generalized coordinate
t = time
α = angle of attack
Δ = residual
η = out-of-phase part of the Lagrangian multiplier
θ = angle
λ = Lagrangian multiplier
μ = $\dot{a}/a$
ξ = in-phase part of the Lagrangian multiplier
χ = roll angle
ω = frequency

Introduction

WING rock is a self-sustaining limit-cycle oscillation (LCO) with a limited amplitude that occurs as a result of nonlinear coupling between the dynamic response and the unsteady aerodynamic forces. High-performance aircraft such as the X-29A have been shown to exhibit wing rock.[1] Reference 2 gives three possible types of wing rock oscillations: conventional wing rock, slender wing rock, and wing–body rock. It is also possible for a low-aspect-ratio rectangular wing to exhibit wing rock.[3] Because the forcing function, i.e., aerodynamic rolling moment, is a nonlinear function of roll angle and its time rate of change, a theoretical prediction of the phenomenon is difficult. For a slender wing with vortex flow separation, a vortex lattice method[4,5] and a discrete vortex model[6] have been used with limited success. For a realistic airplane configuration in wing or body rock, no theoretical prediction of the forces and moments causing the phenomenon has been presented. Therefore, the primary sources of information are wind-tunnel data in free-to-roll testing. In testing, it is useful to determine the forcing function for the purpose of later simulation.

There has been a constant effort for determining the aerodynamic models in wing rock from flight-test or wind-tunnel measurement. The primary difficulty in the identification of aerodynamic models lies in the nonlinear characteristics of the dynamic system. The model identification of wing rock has been developed mostly from physical insight and is not systematic. In fact, the wing rock aerodynamic models have been mostly constructed, not identified, in the past from data sources other than the free-to-roll tests.[7,8] Most of the free-to-roll tests have been conducted to determine the angles of attack within which wing rock occurred. In Ref. 5, the aerodynamic model structure was extensively discussed, but not the parameter identification problem. The existing parameter estimation methods, such as the equation error method,[9] output error method,[10,11] maximum likelihood method,[12] or a combination of some of these methods,[13] have been applied mainly in estimating the aircraft aerodynamic parameters in relatively slow motions. The frequency-domain estimation methods for aerodynamic parameters are not as widely used as the time-domain methods and are usually applicable only to the linear system equations.[14,15] Some common features of these methods are the assumption of some functional forms in the model equation and minimization of a cost function in the time domain to determine the independent parameters of the model equation. To the knowledge of the authors, results from applying the aforementioned estimation methods to the wing rock free-to-roll data have not been reported.

The objective of this paper is to present a nonlinear model estimation method based on minimizing a continuous cost function without assuming a functional form for the forcing function in the estimation process. The estimated forcing function will then be fitted with the assumed model equations in minimal computing time. The optimality equations are solved in the frequency domain to take advantage of the fact that the system frequency in LCO is nearly constant. Application to an aircraft model in free-to-roll testing is then presented.

Received July 18, 1996; revision received Feb. 25, 1997; accepted for publication April 10, 1997.

*Supervisor, Aerodynamics Department, P.O. Box 90008-11-1.
†Bellows Distinguished Professor, Department of Aerospace Engineering. Associate Fellow AIAA.

Theoretical Development

Derivation of Governing Equations

Because the LCO in free-to-roll testing is primarily a single-degree-of-freedom oscillation, a scalar equation will be used to illustrate the derivation. The equation of motion is written in a state variable form, with q being the generalized motion variable:

$$\dot{q} = v, \qquad \dot{v} = F(t) = C_1 q + C_2 \dot{q} + f(t) \tag{1}$$

with initial conditions

$$q(0) = q_0, \qquad v(0) = v_0$$

In Eq. (1), $f(t)$ can be viewed as a control function to be determined by an optimal control theory subject to the constraint of satisfying the dynamic equation (1). It will account for the nonlinearities in the forcing function. The coefficients C_1 and C_2 are constants to be assumed in the estimation process to help numerical convergence, as will be shown later. The forcing function $F(t)$ is calculated as a function of t.

Assume $q_d(t)$ represents the measured response of wing rock. A double differentiation of $q_d(t)$ can produce an estimate of the forcing function. However, the results would be uncertain and exhibit noisy time variation. What is needed is to determine a forcing function $f(t)$ that produces a system response to match $q_d(t)$ as closely as possible, taking into account possible measurement uncertainties. Thus, the problem at hand is a tracking problem in optimal control theory. The forcing function is obtained by forcing the displacement and velocity to follow the specified $q_d(t)$ and $\dot{q}_d$. Therefore, the cost function to be minimized is defined as

$$J = \frac{1}{2}\int_0^{t_f} \left[(\dot{q} - \dot{q}_d)^2 + (q - q_d)^2 + f^2\right] \mathrm{d}t \tag{2}$$

Note that $\dot{q}_d$ is typically not measured. In the present case, only the time derivative of the amplitude is needed and will be calculated by a central difference scheme, as will be shown in the method summary section. To minimize the cost function [Eq. (2)] subject to the constraint [Eq. (1)], the following Hamiltonian must be minimized:

$$H = (\dot{q} - \dot{q}_d)^2 + (q - q_d)^2 + f^2 + \lambda_1 v + \lambda_2 (C_1 q + C_2 \dot{q} + f)$$

$$\lambda_1(t_f) = 0, \qquad \lambda_2(t_f) = 0 \tag{3}$$

where λ_1 and λ_2 are the Lagrangian multipliers. The necessary optimality conditions are, in addition to Eq. (1),

$$\dot{\lambda}_1 = -\frac{\partial H}{\partial q} = -2(q - q_d) - C_1 \lambda_2 \tag{4}$$

$$\dot{\lambda}_2 = -\frac{\partial H}{\partial v} = -2(\dot{q} - \dot{q}_d) - \lambda_1 - C_2 \lambda_2 \tag{5}$$

$$\frac{\partial H}{\partial f} = 2f + \lambda_2 = 0 \tag{6}$$

From Eq. (6), the forcing function $f(t)$ can be obtained as

$$f = -\lambda_2 / 2 \tag{7}$$

Equations (1), (4), and (5) are coupled nonlinear equations with initial conditions for q and final conditions ($t_f \to \infty$) for λ_1 and λ_2. Because the conditions are imposed at two different points, these equations cannot be easily integrated. For a two-point boundary-value problem, flooding or successive linearization[16] is a possible way to obtain the solution. However, in integration using these schemes, the solution is very sensitive to a small change in the unspecified initial conditions. Therefore, long computational time is expected even if the solution converges. For the present purpose, we will first reduce these equations to the frequency domain by Beecham–Titchener's method[17] (B–T method) and eliminate λ_1 and λ_2 from the resulting equations. The B–T method has been used successfully in the past.[18]

B–T Method

Periodic motions can be expressed by pure sinusoidal functions. Assume a trial solution in the form of

$$q = a \cos\theta \tag{8}$$

where both a and θ are functions of t. The solutions of the Lagrangian multipliers are expected to consist of an in-phase part, i.e., $\cos\theta$ term, and an out-of-phase part, i.e., $\sin\theta$ term, and so the following forms for λ_1 and λ_2 are assumed:

$$\lambda_1 = a(\xi_1 \sin\theta + \eta_1 \cos\theta) \tag{9}$$

$$\lambda_2 = a(\xi_2 \sin\theta + \eta_2 \cos\theta) \tag{10}$$

where a, θ, ξ_1, η_1, ξ_2, and η_2 are functions of t. Differentiating Eqs. (8–10), it follows that

$$\dot{q} = a(\mu \cos\theta - \omega \sin\theta) \tag{11}$$

$$\ddot{q} = a[(\mu^2 - \omega^2 + a\mu\mu')\cos\theta - (2\mu\omega + a\mu\omega')\sin\theta] \tag{12}$$

$$\dot{\lambda}_1 = a\{[\mu(\eta_1 + a\eta_1') + \omega\xi_1]\cos\theta + [\mu(\xi_1 + a\xi_1') - \omega\eta_1]\sin\theta\} \tag{13}$$

$$\dot{\lambda}_2 = a\{[\mu(\eta_2 + a\eta_2') + \omega\xi_2]\cos\theta + [\mu(\xi_2 + a\xi_2') - \omega\eta_2]\sin\theta\} \tag{14}$$

where $\mu = \dot{a}/a$, $\omega = \dot{\theta}$, and $(\,)' = \mathrm{d}(\,)/\mathrm{d}a$. As a first approximation, it is assumed in accordance with the B–T method that

$$\mu' = \omega' = \xi_1' = \eta_1' = \xi_2' = \eta_2' = 0$$

Substituting Eqs. (8), (11), and (12) into Eq. (1), the following two equations are obtained by the harmonic averaging method[18]:

$$\mu^2 - \omega^2 = C_1 + C_2\mu - \eta_2/2 \tag{15}$$

$$2\mu\omega = C_2\omega + \xi_2/2 \tag{16}$$

To eliminate λ_1 and λ_2, we first obtain from Eqs. (4), (8), and (13)

$$(\mu\xi_1 - \omega\eta_1 + C_1\xi_2)\sin\theta + (\mu\eta_1 + \omega\xi_1 + 2 + C_1\eta_2)\cos\theta = 2q_d/a \tag{17}$$

In Eq. (17), $q_d(t)$ is known. To apply the averaging method, $q_d(t)$ must be expressed in terms of $\sin\theta$ and $\cos\theta$. Therefore, q_d is taken to be

$$q_d = A(t)\cos\theta \tag{18}$$

Time differentiation of Eq. (18) gives

$$\dot{q}_d = \dot{A}\cos\theta - A\omega\sin\theta \tag{19}$$

Equation (17) can again be separated into the in-phase and out-of-phase components by harmonic averaging:

$$\mu\eta_1 + \omega\xi_1 = -2(1 - A/a) - C_1\eta_2 \tag{20}$$

$$\mu\xi_1 - \omega\eta_1 = -c_1\xi_2 \tag{21}$$

Similarly, substituting Eqs. (8), (11), (18), and (19) into Eq. (5) and applying the averaging method,

$$\xi_1 = 2\omega(1 - A/a) - (\mu + C_2)\xi_2 + \omega\eta_2 \tag{22}$$

$$\eta_1 = -2(\mu - \dot{A}/a) - (\mu + C_2)\eta_2 - \omega\xi_2 \tag{23}$$

The preceding two equations can be used to eliminate ξ_1 and η_1 from Eqs. (20) and (21). It follows that

$$[-2\mu\omega - C_2\omega]\xi_2 + \left(\omega^2 - \mu^2 - C_2\mu + C_1\right)\eta_2 = -2(1 + \omega^2)(1 - A/a) + 2\mu(\mu - \dot{A}/a) \tag{24}$$

$$\left(\omega^2 - \mu^2 + C_1 - C_2\mu\right)\xi_2 + (2\mu\omega + C_2\omega)\eta_2 = -2\mu\omega(1 - A/a) - 2\omega(\mu - \dot{A}/a) \tag{25}$$

In Eqs. (24) and (25), there are still terms representing the effect of Lagrangian multipliers, i.e., ξ_2 and η_2. To eliminate these, Eqs. (15) and (16) are solved for ξ_2 and η_2 to give

$$\xi_2 = 2(2\mu\omega - C_2\omega) \tag{26}$$

$$\eta_2 = 2\left(\omega^2 - \mu^2 + C_1 + C_2\mu\right) \tag{27}$$

Substituting ξ_2 and η_2 into Eqs. (24) and (25) gives

$$d_{11}h_1 + d_{12}h_2 = -\mu\omega(1 - A/a) - \omega(\mu - \dot{A}/a) \tag{28}$$

$$d_{21}h_1 + d_{22}h_2 = -(1 + \omega^2)(1 - A/a) + \mu(\mu - \dot{A}/a) \tag{29}$$

In these final equations to be solved [Eqs. (28) and (29)], the Lagrangian multipliers ξ_1, η_1, ξ_2, and η_2 have all been eliminated. Because $\mu = \dot{a}/a$ and $\omega = \dot{\theta}$, Eqs. (28) and (29) represent a set of nonlinear implicit ordinary differential equations of the form

$$G(y', y) = 0 \tag{30}$$

where G is a two-dimensional function and $y' = (\dot{a}, \dot{\theta})^T$, $y = (a, \theta)^T$, and the initial conditions a_0 and θ_0 can be obtained from q_0 and v_0. Equation (30) with specified initial conditions can be solved by an existing code, DASSL,[19] using the approach of backward differentiation formulas. A summary of the method is given in Ref. 18.

Summary of the Present Method

The resulting optimal estimation equations [Eqs. (28) and (29)] are integrated for $a(t)$ and $\theta(t)$. From Eqs. (26) and (27), ξ_2 and η_2 are then determined. From Eqs. (7) and (10), the estimated forcing function is obtained:

$$f(t) = -(a/2)(\xi_2 \sin\theta + \eta_2 \cos\theta) \tag{31}$$

The forcing function $F(t)$ is the sum of the C terms and $f(t)$. Finally, a model equation is assumed for $F(t)$. In assuming a model equation in terms of the state variables, it is preferred not to use spline functions so that the stability parameters, such as the roll damping derivative, can be directly identified. In the frequency domain, it is sufficient to assume the following algebraic model:

$$\begin{aligned} F(t) = {} & D_1\chi + D_2\dot{\chi} + D_3\dot{\chi}|\chi| + D_4\chi^2 + D_5\chi\dot{\chi} \\ & + D_6\dot{\chi}^2 + D_7\chi^3 + D_8\chi^2\dot{\chi} + D_9\chi\dot{\chi}^2 + D_{10}\dot{\chi}^3 \\ & + \cdots + C_m\chi^n + \cdots + C_{m+n}\dot{\chi}^n \end{aligned} \tag{32}$$

This equation is fitted to the estimated $F(t)$ through the least-squares method. Note that D_2 is related to the roll damping derivative and is not necessarily equal to C_2 in Eq. (1). The nonanalytic term, i.e., the D_3 term, is assumed because, based on the physical consideration, the roll damping in sideslip is independent of the sign of sideslip.[7]

The computational algorithm is summarized as follows.

1) The starting time in the test data to be used is typically one at which the reading is at a peak, i.e., the initial point is at a peak of a cosine curve.

2) The amplitude A at any time t is obtained by using successive peak values and the corresponding times. Within these time intervals, the amplitude A at any time t is obtained by Lagrange's interpolation method.

3) The time rate of change in amplitude $\dot{A}$ is calculated by numerical differentiation with a second-order central difference scheme. The scheme is based on an uneven spacing.

4) The time lapse between two successive peaks represents a local period of the oscillation. The reciprocal of the period is the local frequency. The frequency ω_d at any time t is then obtained by interpolation of these local frequency data. A fast Fourier transform program, DFT, can also be used to find ω_d.

5) C_1 in Eqs. (28) and (29) is set equal to $-\omega_d^2$ and $C_2 = 2\dot{A}/A$ when the DASSL program is used to integrate Eqs. (28) and (29).

6) The initial values a_0, $\dot{a}_0$, θ_0, and ω_0 for the integration in DASSL should be consistent, i.e., they must satisfy the implicit differential equations. The values obtained in steps 3 and 4 may be used as the initial trial values.

7) For the oscillation with a nonzero trim point, the mean value q_m of the data should be determined first. The mean value is taken to be the arithmetic average of the data and is automatically determined in the program DFT. The present code will subtract the mean values from the time-history data at the beginning of the estimation process and add them back after the solution is completed.

Numerical Results and Discussion

The present estimation algorithm will be verified with a specific mathematical model for wing rock of an 80-deg delta wing.[7,18] After verification, the method will be applied to an airplane configuration in a free-to-roll testing that was conducted in the Aero Industry Development Center 7 × 10 ft low-speed wind tunnel in Taiwan.

80-deg Delta Wing

The time-history data of roll angle was generated through Runge–Kutta numerical integration of the following wing rock model equation:

$$\ddot{\chi} = -26.6667\chi + 0.76485\dot{\chi} - 2.92173\dot{\chi}|\chi| \tag{33}$$

This model equation will serve as a baseline to study the effects of the assumed values of constant coefficients C_1 and C_2 in Eq. (1) on numerical convergence. This is because the system of equations to be solved [Eqs. (28) and (29)] is nonlinear so that the convergence of its solution depends on the initial estimates. The effects of integration step size and error tolerance in DASSL on the estimated results have also been examined. It is found that by setting $C_1 = -\omega_d^2$ and $C_2 = 2\dot{A}/A$, the present scheme would converge better. In Eq. (32), D_n with $n \geq 4$ are set to zero in the present case. By varying the time step size Δt with a fixed error tolerance being 10^{-6}, the estimated model constants and the corresponding least-square error in fitting the forcing function are presented in Table 1. It is seen that the smaller the time step size, the more accurate the least-square fit. As for the accuracy of the parameters estimated, for the worst case, the percentage error for D_3 is 0.1% for $\Delta t = 0.005$ and 2.8% for $\Delta t = 0.025$. The selection of the step size depends on the desired accuracy of the solution and the available computational time. In the following applications, $\Delta t = 0.025$ will be used.

Airplane Configuration in Free-to-Roll Testing

The model is the clean configuration used in Ref. 20. The model was mounted on a roll axis, which was free to roll. The model will not roll until a critical angle of attack is reached. The test data to be analyzed are for the fuselage–vertical tail combination at zero sideslip and a dynamic pressure equal to 31.1 psf.

The experimental data for the time history of roll angle are shown in Fig. 1. It is seen that the oscillation is centered at a roll angle of −0.24 rad (−13.75 deg). At other test conditions, it is possible that the oscillation may be centered about 0 deg. This phenomenon of wing or body rock about more than one roll angle has been defined as having multiple roll attractors.[21] It has been shown to exist also on 65-deg delta wings.[22,23]

The current estimation algorithm is for a symmetric oscillation about $\chi = 0$. Therefore, the mean value of the oscillation time history is subtracted before applying the algorithm. By taking the fast Fourier transform of the time history data, the main frequency can be shown to be around 11.5 rad/s. After the forcing function, i.e., the rolling moment, is estimated, polynomials of different degrees are examined in the least-square fit. The results are shown in Table 2,

Table 1 Models obtained by using different integration step sizes

Δt, s	D_1	D_2	D_3	Least-square error
0.005	−26.664	0.764	−2.918	1.79×10^{-10}
0.010	−26.655	0.761	−2.906	8.55×10^{-9}
0.020	−26.619	0.749	−2.861	1.09×10^{-7}
0.025	−26.592	0.741	−2.826	6.03×10^{-6}
Correct model	−26.667	0.765	−2.922	

Table 2 Linear terms obtained by using polynomials of different degrees (with $D_3 \neq 0$)

Degree of polynomials	D_1	D_2	Least-square error
1	−130.6	1.06	1.12×10^{-3}
2	−130.4	1.08	7.66×10^{-4}
3	−145.4	2.14	6.71×10^{-4}
4	−145.3	2.03	6.32×10^{-4}
5	−135.1	1.12	3.48×10^{-4}

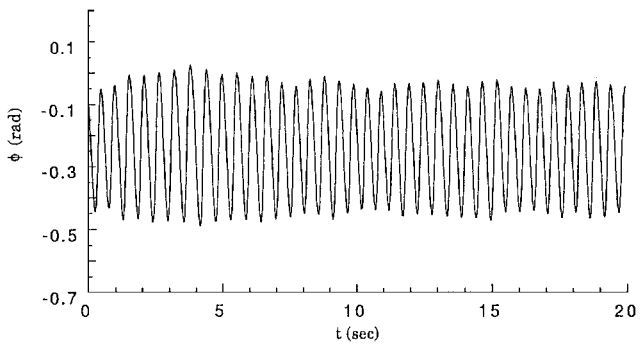

Fig. 1 Free-to-roll data of a fuselage–vertical tail configuration from a low-speed tunnel, α = 33 deg and M = 0.15.

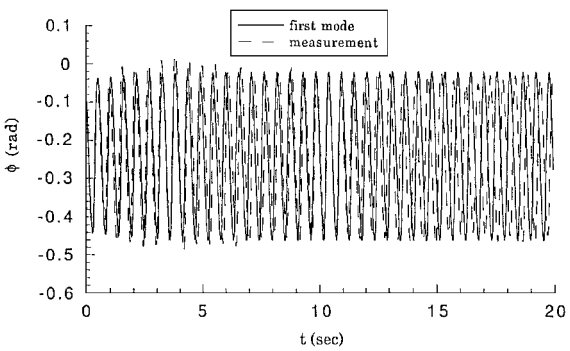

Fig. 2 Comparison of roll angle response based on the first mode of estimated aerodynamic model with free-to-roll data.

which shows that the first two parameters D_1 and D_2 converge to approximately the same values for the first-degree and the second-degree polynomials. The second-degree polynomial has smaller least-square error than the first-degree one. Although the fifth-degree polynomials have the least error, the second-degree model is selected for simplicity. A more precise method for determining the appropriate degree of polynomials is the stepwise regression method.[24]

In Ref. 5, using only the analytical terms in the model equation was favored. Therefore, the model with $D_3 = 0$ is also used to fit the estimated rolling moment. The results (not shown) show that the values of D_1 and D_2 are not convergent as the degree of polynomials is increased.[25]

Just like Fourier analysis of any function, the estimated forcing function can be fitted successively with modes of different frequencies. The model equation of the first mode is estimated, based on the polynomial of degree 2, to be

$$F_1(t) = -130.414\chi_1 + 1.081\dot{\chi}_1 - 11.553\dot{\chi}_1|\chi_1| + 43.390\chi_1^2 - 0.711\chi_1\dot{\chi}_1 - 0.248\dot{\chi}_1^2 \quad (34)$$

The computed response of mode 1 is shown in Fig. 2, which shows a fair agreement with experimental data. The slight phase shift is due to the effect of higher-frequency components. The estimated rolling moment is shown in comparison with the result of least-squares fit in Fig. 3. The match of phase angle is good, but the amplitude of the resulting response from the least-square-fit model is slightly smaller than the estimated one. The aerodynamic model

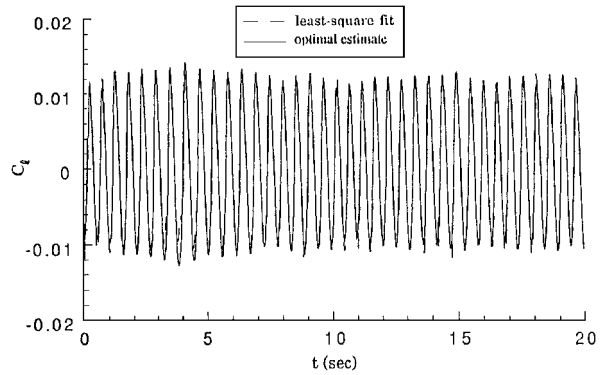

Fig. 3 Estimated rolling moment coefficient with a least-squares fit of a model equation.

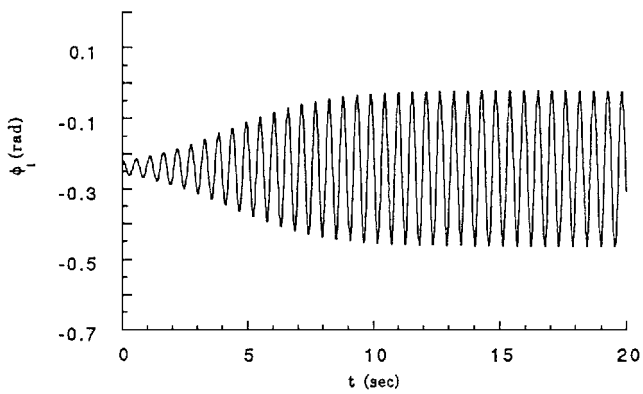

Fig. 4 Simulation of body rock of a fuselage–vertical tail configuration based on the first mode of estimated aerodynamic model.

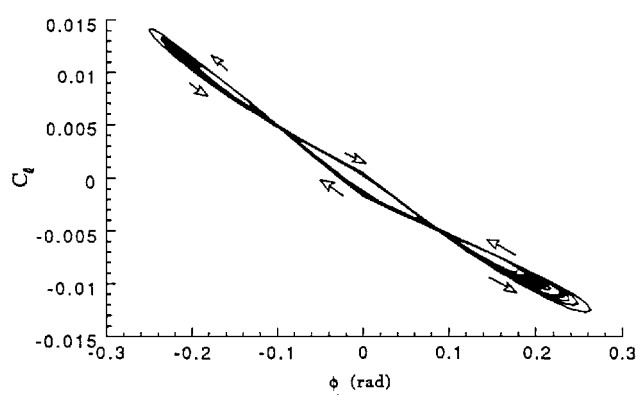

Fig. 5 Hysteresis loop based on the first mode of estimated aerodynamic model for a fuselage–vertical tail configuration.

that is estimated from the fully developed LCO data can exhibit proper transient response as shown in Fig. 4, which shows the response of the model to a small initial disturbance. For a linear model, the maximum response would be proportional to the initial disturbance. The hysteresis loop of the first mode oscillation is shown in Fig. 5, which is similar to the hysteresis loop of the 80-deg delta wing. During the oscillation, the energy gained in the center clockwise loop caused by the negative damping, i.e., a positive D_2, is balanced by the energy dissipated in the outer counterclockwise loops.

To determine whether the predicted response in Fig. 2 can be improved, the difference between the predicted and measured responses, defined as the residual, is fitted with a second mode. However, the improvement by adding a second mode is found to be small.[25] Therefore, for a practical purpose, the body rock motion for the present fuselage–vertical tail configuration in free-to-roll tests can be described as an oscillatory motion with a single dominant frequency.

Application of Estimated Aerodynamic Model

Once the aerodynamic model is estimated, the same model can be used in improving the system response as long as the aerodynamic configuration remains the same. One example of system modifications to improve the response is the design of feedback control. In application to a control system design, mechanical or artificial damping can be added to the estimated model to improve the behavior of system response. For example, the value of the linear damping D_2 can be changed from $+1.08$ per second to a negative value, i.e., stable, by a conventional roll damper, control surfaces such as aileron and rudder, or forebody jet blowing for aircraft at high angles of attack. In Ref. 18, an optimal roll rate feedback was determined to be effective in suppressing wing rock of an 80-deg delta wing.

One important difference in wing rock of the 80-deg delta wing and the body rock of the fuselage–vertical tail combination is that increasing the system stiffness may eliminate the body rock but not the wing rock. Change in stiffness affects the values of D_1. The model simulation of the 80-deg delta wing with different values of D_1 is shown in Fig. 6. Wing rock with a larger value of D_1 oscillates at a higher frequency but with the same amplitude. On the other hand, the body rock as shown in Fig. 7 shows that increasing the stiffness will increase the frequency of the oscillation and also may suppress the oscillation. This is because the system damping μ is affected by C_1, which is nearly equal to D_1 [Eqs. (28) and (29)]. With C_1 large enough, μ becomes largely negative. This was not true for the 80-deg delta wing. System stiffness can be increased by using roll angle feedback.

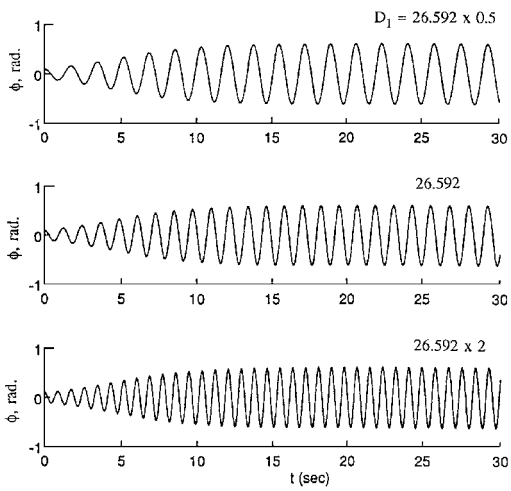

Fig. 6 Model simulation of wing rock for an 80-deg delta wing with various values of D_1, s^{-2}.

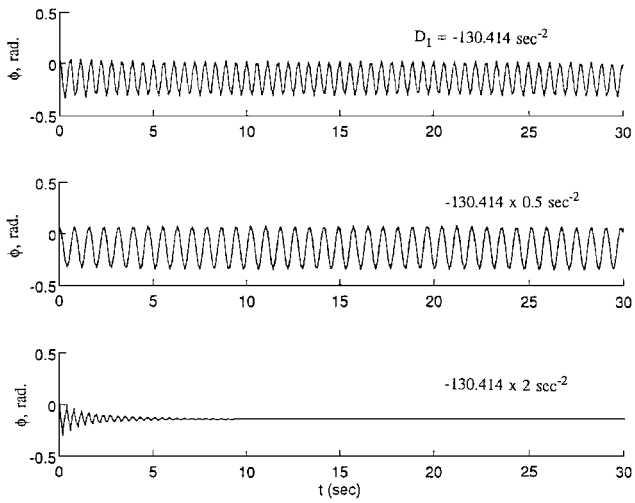

Fig. 7 Model simulation of body rock for the fuselage–vertical tail configuration with various values of D_1, s^{-2} and $D_2 = 1.081$ s^{-1}.

Conclusions

A method to estimate the aerodynamic forcing function in wing or body rock motions has been developed. The method was based on an optimal estimation theory in the frequency domain. The method used a continuous cost function, which was a measure of the difference between the estimated states and the measured data. Simplification of the optimality equations through the B–T averaging method allowed the Lagrangian multipliers to be eliminated from the equations to be solved. The forcing function thus obtained was fitted with state variables and their products through a least-squares method. The model candidate selection was based on the least-squares error and the simplicity of the form.

The method was verified with a wing rock model for an 80-deg delta wing. It was then used to estimate the rolling moment coefficient for a fuselage–vertical tail configuration in free-to-roll testing. The resulting aerodynamic model produced fair agreement in oscillation characteristics as compared with the measured data. It was also shown that adding damping would damp the LCO of both the 80-deg delta wing and the fuselage–vertical tail combination as expected. The amount of damping needed to damp out the LCO could be determined by the estimated aerodynamic models. Additional stiffness also was shown to damp the LCO of the fuselage–vertical tail model but not the 80-deg delta wing.

References

[1] Fratello, D. J., Croom, M. A., Nguyen, L. T., and Domack, C. S., "Use of the Updated NASA Langley Radio-Controlled Drop-Model Technique for High-α Studies of the X-29A Configuration," AIAA Paper 87-2559, Aug. 1987.

[2] Ericsson, L. E., "Various Sources of Wing Rock," *Journal of Aircraft*, Vol. 27, No. 6, 1990, pp. 488–494.

[3] Levin, D., and Katz, J., "Self-Induced Roll Oscillation of Low-Aspect-Ratio Rectangular Wings," *Journal of Aircraft*, Vol. 29, No. 4, 1992, pp. 698–702.

[4] Elzebda, J. M., Mook, D. T., and Nayfeh, A. H., "Influence of Pitching Motion on Subsonic Wing Rock of Slender Delta Wings," *Journal of Aircraft*, Vol. 26, No. 6, 1989, pp. 503–508.

[5] Elzebda, J. M., Nayfeh, A. H., and Mook, D. T., "Development of an Analytical Model of Wing Rock for Slender Delta Wings," *Journal of Aircraft*, Vol. 26, No. 8, 1989, pp. 737–743.

[6] Arena, A. S., and Nelson, R. C., "A Discrete Vortex Model for Predicting Wing Rock of Slender Wings," AIAA-92-4497, Aug. 1992.

[7] Nguyen, L. T., Yip, L., and Chambers, J. R., "Self-Induced Wing Rock of Slender Delta Wings," AIAA Paper 81-1883, Aug. 1981.

[8] Suarez, C. J., Smith, B. C., and Malcolm, G. N., "Experimental and Numerical Analysis of the Wing Rock Characteristics of a 'Wing-Body-Tail' Configuration," AIAA Paper 93-0187, Jan. 1993.

[9] Aksteter, J. W., Parks, E. K., and Bach, R. E., Jr., "Parameter Identification and Modeling of Longitudinal Aerodynamics," *Journal of Aircraft*, Vol. 32, No. 4, 1995, pp. 726–731.

[10] Maine, R. E., and Iliff, W. K., "Application of Parameter Estimation to Aircraft Stability and Control—The Output-Error Approach," NASA Reference Publication 1168, June 1986.

[11] Preissler, H., and Schäufele, H., "Equation Decoupling—A New Approach to the Aerodynamic Identification of Unstable Aircraft," *Journal of Aircraft*, Vol. 28, No. 2, 1991, pp. 146–150.

[12] Iliff, K. W., and Maine, R. E., "Maximum Likelihood Estimation with Emphasis on Aircraft Flight Data," *JPL Proceedings of the Workshop on Identification and Control of Flexible Space Structures*, Vol. 3, Jet Propulsion Lab., California Inst. of Technology, Pasadena, CA, 1985, pp. 197–246.

[13] Trankle, T. L., and Bachner, S. D., "Identification of a Nonlinear Aerodynamic Model of the F-14 Aircraft," *Journal of Guidance, Control, and Dynamics*, Vol. 18, No. 6, 1995, pp. 1292–1297.

[14] Klein, V., "Estimation of Aircraft Aerodynamic Parameters from Flight Data," *Progress in Aerospace Sciences*, Vol. 26, No. 1, Pergamon, New York, 1989, pp. 1–77.

[15] Raisinghani, S. C., and Goel, A. K., "Frequency-Domain Application of Gauss-Newton Method to Extract Aircraft Longitudinal Parameters," *Aeronautical Journal*, Vol. 90, No. 891, 1986, pp. 27–34.

[16] Citron, S. J., *Elements of Optimal Control*, Holt, Reinhart, and Winston, New York, 1969, pp. 109–112.

[17] Beecham, L. T., and Titchener, I. M., "Some Notes on an Approximate Solution for the Free Oscillation Characteristics of Non-Linear System Typified by $\ddot{X} + F(X, \dot{X}) = 0$," British Aeronautical Research Council, Repts. and Memoranda 3651, London, Aug. 1969.

[18] Luo, J., and Lan, C. E., "Control of Wing-Rock Motion of Slender Delta Wings," *Journal of Guidance, Control, and Dynamics*, Vol. 16, No. 2, 1993, pp. 225–231.

[19]Brenan, K. E., Campbell, S. L., and Petzold, L. R., *Numerical Solution of Initial-Value Problem in Differential-Algebraic Equations*, Elsevier Science, New York, 1989.

[20]Fu, A. K., Lan, C. E., and Shyu, L. S., "An Experimental Investigation of the Effect of Leading-Edge Extensions on Directional Stability and the Effectiveness of Forebody Nose Strakes," AIAA Paper 92-2715, June 1992.

[21]Williams, D. L., and Nelson, R. C., "Influence of Wing-Forebody Separation on Forebody-Induced/Driven Wing Rock," AIAA Paper 95-3441, Aug. 1995.

[22]Hanff, E. S., and Jenkins, S. B., "Large-Amplitude High-Rate Roll Experiments on a Delta and Double Delta Wing," AIAA Paper 90-0224, Jan. 1990.

[23]Hanff, E. S., and Ericsson, L. E., "Multiple Roll Attractors of a Delta Wing at High Incidence," AGARD-CP-494, Paper 31, July 1991, pp. 31-1–31-10.

[24]Batterson, J. G., and Klein, V., "Parameter Identification Applied to the Oscillatory Motion of an Airplane Near Stall," *Journal of Aircraft*, Vol. 21, No. 7, 1984, pp. 498–504.

[25]Tan, S. Y., "Identification of Aerodynamic Models in Limit-Cycle Oscillations," Ph.D. Dissertation, Dept. of Aerospace Engineering, Univ. of Kansas, Lawrence, KS, Jan. 1996.